Molecular Electronics

DOI: 10.1002/ange.200806028

Spectroscopic Tracking of Molecular Transport Junctions Generated by Using Click Chemistry**

Xiaodong Chen, Adam B. Braunschweig, Michael J. Wiester, Sina Yeganeh, Mark A. Ratner, and Chad A. Mirkin**

The development of efficient methods for the construction of molecular transport junctions (MTJs) and the ability to spectroscopically identify molecules assembled within the junctions continues to challenge the field of molecular electronics.[1,2] Most of the current work in MTJ fabrication relies primarily on ex situ syntheses of molecular wires (e.g., dithiolated molecules) followed by subsequent insertion of the molecules into the gap devices.[3] The problems associated with this approach are: 1) the difficulty involved in synthesizing long molecular wires with thiol groups on both ends because of the low solubility and reaction yields of these molecules and 2) complications in bridging the electrodes because of a strong tendency of such molecular wires to aggregate.[4] In addition, the small junction sizes (normally only several nanometers wide) often prohibit the use of routine spectroscopic tools to identify the contents of MTJs. Therefore, a modular method for the in situ synthesis of molecular wires to bridge nanogaps,[4,5] which allows spectroscopic tracking of the assembly process, merits development. Herein, we report a new method for the fabrication of MTJs by using the alkyne–azide "click reaction" within nanogaps fabricated by on-wire lithography (OWL), while using surface-enhanced Raman scattering (SERS) to characterize the assembly processes within the gaps. This strategy for forming MTJs proceeds in high yields, and, as a result of the accessible functional-group requirements of click chemistry, is a modular approach that can be used to form MTJs comprising different molecular components. Additionally, this approach is well-suited for studying the transport properties of various molecular architectures because the resulting triazole formed by the reaction of the alkyne and azide groups retains the conjugation required for electronic transport.

OWL is an electrochemistry-based nanofabrication technique used to prepare a wide variety of nanowire-based structures (e.g., nanogaps and disk arrays) with control over composition and morphology.[6] The obtained structures have been used for prototyping nanostructured materials with advanced functions in the context of molecular electronics[6–8] and SERS.[9–11] OWL allows the preparation of gaps with feature-size control down to 2 nm, which makes them promising testbeds for the fabrication of MTJs.[7] The characteristics of OWL-fabricated nanogaps include high-throughputs and tunable, molecular-sized features. Herein, we use click chemistry for the in situ modular synthesis of molecular wires within the OWL-fabricated nanogaps. Click chemistry is a synthetic approach popularized by Sharpless and co-workers that involves reactions that proceed quickly, with high yields and specificity, under mild conditions.[12] An advantage of forming molecular wires by using the click methodology within the OWL-fabricated nanogaps is that in situ fabrication within a confined space (nanogap) is challenging for other existing testbeds, such as scanning probes[13–15] and wire crossing,[16] because these techniques are not easily solution-processable. On the other hand, mechanical break-junction techniques[17,18] provide only limited control over gap size in comparison with nanogaps formed by OWL. In this study, the copper(I)-catalyzed 1,3-dipolar Huisgen cycloaddition reaction (click reaction) between azide and alkyne groups (Figure 1c) is utilized as a model reaction for preparing molecular wires within OWL-fabricated nanogaps to form MTJs.

The general scheme for bridging the nanogaps by using click chemistry for MTJ fabrication is shown in Figure 1a. In a typical experiment, 4-ethynyl-1-thioacetylbenzene (**1**)[19] is first assembled into a monolayer on the surfaces of the

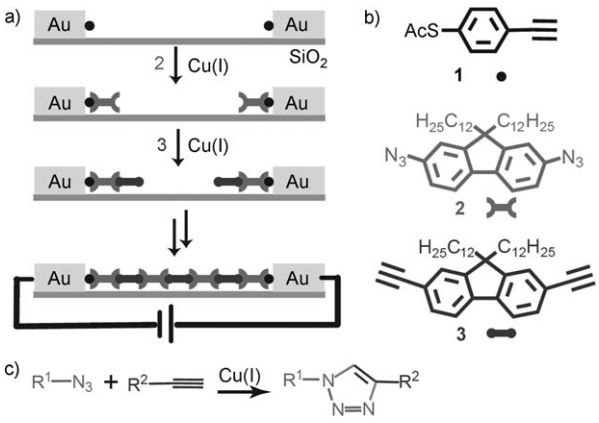

Figure 1. a) Schematic illustration of click chemistry within the nanogaps. b) Molecules used in this study. c) The alkyne–azide click reaction.

[*] Dr. X. Chen,[+] Dr. A. B. Braunschweig,[+] M. J. Wiester,[+] S. Yeganeh, Prof. M. A. Ratner, Prof. C. A. Mirkin
Department of Chemistry and
International Institute for Nanotechnology, Northwestern University
2145 Sheridan Road, Evanston, IL 60208 (USA)
E-mail: ratner@northwestern.edu
chadnano@northwestern.edu

[+] These authors contributed equally to this work.

[**] C.A.M. acknowledges support from the NUNSF-NSEC. and for an NSSEF Fellowship from the Department of Defense. A.B.B. is grateful for an NIH Postdoctoral Fellowship. S.Y. thanks the ONR for an NDSEG fellowship. M.A.R. acknowledges funding from the MRSEC at NU.

Supporting information for this article is available on the WWW under http://dx.doi.org/10.1002/anie.200806028.

electrodes, which are located at opposite ends of an OWL-fabricated nanogap, by immersing the entire device in a solution of **1** (1 mM) in dichloromethane/methanol (2:1, v/v) for 12 h. Concentrated sulfuric acid (50 μL) is added to the solution to deprotect the thiol groups.[20] The device is rinsed with dichloromethane/methanol, chloroform, and ethanol, and then immersed in a solution of 2,7-di-azido-fluorene[21] (**2**; 1 mM) in DMF (10 mL) containing a solution (200 μL) of copper sulfate (0.074 M) and ascorbic acid (0.148 M). One of the azide groups in compound **2** reacts with the alkyne group on electrode-immobilized **1** to form a 1,2,3-triazole unit at one end, whilst the azide group at the other end is left unchanged. This structure can be further extended by reaction with 2,7-diethynyl-fluorene (**3**),[21] which, in turn, can be reacted again with **2**. Following the appropriate number of reaction cycles, the molecular wires that grow from the opposing electrodes combine and bridge the nanogap. The point at which the bridge is formed can be determined from the *I–V* characteristics of the device, and the number of reaction steps required to form a bridge depends on the size of the gap.

As a proof of concept, we first attempted a one-step click reaction with **1** and **2** to bridge a 2 nm OWL-fabricated gap and form MTJs. The calculated S–S distance of the target bridging molecule is 2.6 nm, which is long enough to span the gap. In a typical experiment, 360 nm diameter wire structures with 2 nm nanogaps (Figure 2a) were cast onto a substrate bearing gold microelectrodes and then connected to the electrodes by electron-beam lithography and subsequent chromium and gold thermal deposition (Figure 2b). The two-terminal *I–V* characteristics of the gap devices were measured at room temperature before and after click reactions (Figure 2c). The empty nanogaps, or nanogaps modified with a monolayer consisting only of **1**, exhibit no conductance within the noise limit of the measurement (< 2 pA; Figure 2c, ■ and △). However, following the click reaction of **1** and **2** within the gap, the *I–V* characteristics show a clear molecular response in the μA range (Figure 2c, ▽), which indicates the realization of a conjugated molecular bridge within the nanogap formed as a result of the click reaction. The yield for working devices is 41% (12 out of 29 devices with $I > 0.1$ nA at 1 V bias). It should be noted that the magnitude of the current measured in different MTJ devices varies from 0.1 nA to 600 μA at 1 V bias, which presumably results from the different numbers of molecules that bridge the nanogap in different experiments (see Figure S5 in the Supporting Information). It is also likely that the roughness of the electrode surface contributes to the observed variation. As a control experiment, we synthesized the dithiol **4** (see the Supporting Information for structure) ex situ from **1** and **2**, and the current amplitude and yield of working devices is lower (ca. 10%, 3 out of 31) than that of MTJ devices assembled in situ. This observation is likely to result from the slow diffusion of the large molecule into the nanogap.[11]

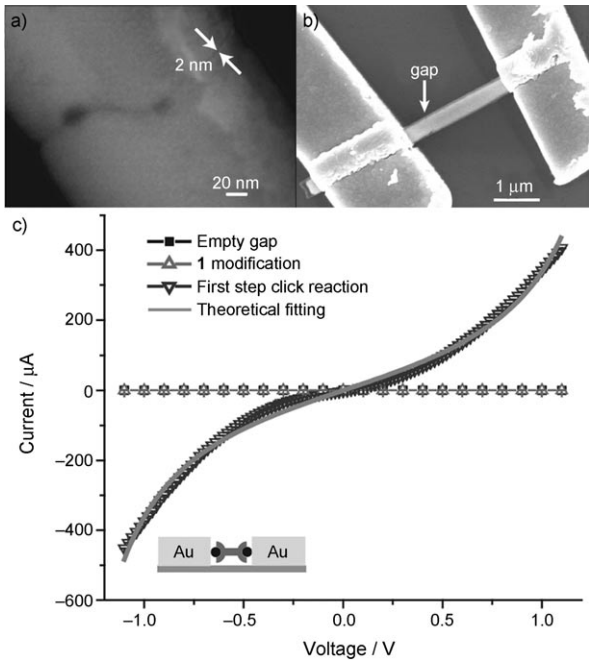

Figure 2. a) SEM image of a 2 nm OWL-fabricated nanogap. b) An SEM image of 2 nm nanogap–MTJ device. c) Representative *I–V* response for 2 nm OWL-fabricated gaps before (■), after (△) modification with **1**, and the bridging click reaction of **2** with **1** (▽). The plain gray line shows the theoretical fitting of the *I–V* curve.

X-ray photoelectron spectroscopy (XPS) of the proof-of-concept system on a bulk surface confirmed that the click reactions proceed on Au substrates. For example, the assembly of **1** and the click reaction between **1** and **2** were carried out on a planar Au substrate surface (model system) and followed by XPS in the S 2p region and the N 1s region. In general, the S 2p spectra are composed of 2p3/2 and 2p1/2 peaks with an intensity ratio of 2:1, as theoretically determined from the spin-orbit splitting effect. Binding peaks at 162.4 (S 2p3/2) and 163.9 eV (S 2p1/2), which are assigned to the bound sulfur atoms, are shown in Figure S3 in the Supporting Information.[22] Furthermore, when a surface-bound monolayer of **1** reacts with **2** in the presence of Cu^I, a peak at 400.2 eV is observed, which arises from the presence of both triazole and azide groups (N 1s).[23] These spectral signatures confirm that the 1,3-dipolar cycloaddition reaction between azide and alkyne groups proceeds successfully on monolayer-modified Au surfaces.

SERS measurements carried out directly on the nanogaps confirm that the click reaction proceeds within these confined spaces. OWL-fabricated nanogaps less than 100 nm in width have been shown to act as Raman "hot spots" with enhancement factors as large as 10^8,[9,11] therefore molecules assembled within nanogaps can be efficiently identified by SERS.[24,25] To evaluate the potential of OWL-fabricated nanogaps for simultaneous assembly and spectroscopic identification, we fabricated sub-100 nm nanogap structures, with Au segments on the opposite sides of the nanogaps. In a typical experiment, the molecules were assembled by click chemistry in a nanogap ((98 ± 11) nm; Figure 3a) as described above for the MTJ fabrication, and the Raman spectra and image of the gap area were measured by confocal scanning Raman microscopy (WiTec Alpha300). For the gap structures modified with **1**, the Raman spectrum (Figure 3c, Spectrum 1) clearly shows the presence of alkyne groups (C≡C symmetric stretch at 2108 cm^{-1}) and benzene rings (aro-

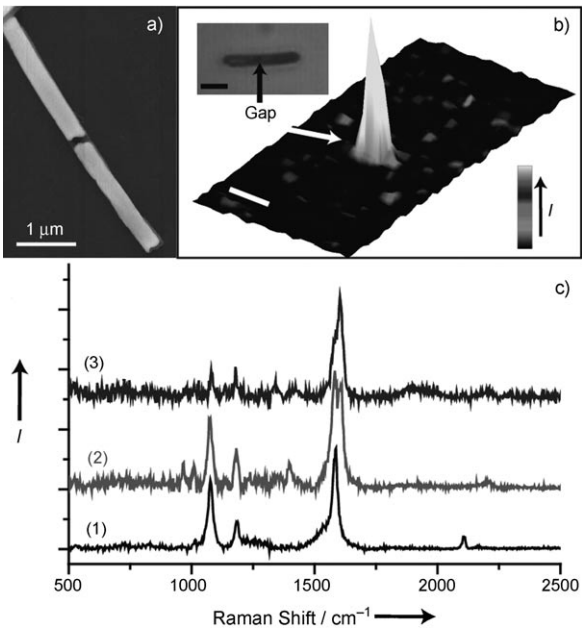

Figure 3. a) SEM image of an OWL-fabricated nanowire with a 100 nm nanogap. b) 3D confocal scanning Raman images of an OWL-fabricated gap structure modified with **1**. The inset shows a simultaneously obtained optical image that shows the position of the nanogap. Scale bar: 2 μm. c) Representative Raman spectrum taken for the different steps: 1) **1** within the gap, 2) following addition of **2**, and 3) following addition of **3**.

matic C–C stretch of **1** at 1585 cm^{-1}). In addition, when compared with the spectrum of the neat solid of **1** (Figure S6 in the Supporting Information), the absence of thioacetyl (634 cm^{-1}) and SH (bending, 915 cm^{-1}) vibration modes indicates Au–S bonding.[26] The confocal Raman images (Figure 3b) obtained by integrating the spectral intensity from 1520 to 1620 cm^{-1} and the bright-field optical image show that the hot spots are localized in the gap. When **2** reacts with the monolayer of **1** under click reaction conditions, new peaks at 967 and 1010 cm^{-1} (the triazole ring stretch),[27] 1606 cm^{-1} (aromatic C–C stretch of **2**), and 2198 cm^{-1} (asymmetric stretching of azide groups) appear, and the peak at 2108 cm^{-1} disappears (Figure 3c, Spectrum 2), which indicates that the click reaction of **1** and **2** proceeded successfully. Furthermore, when **3** reacts with **2** under click reaction conditions, the relative intensity of the peak at 1606 cm^{-1} increases (Figure 3c, Spectrum 3), which confirms the occurrence of the reaction between **3** and **2**. These SERS experiments demonstrate the direct observation of the chemical reactions within nanogaps and, as a result, confirm the chemical composition of the molecules confined within the MTJs.

Theoretical calculations were performed to characterize the transport behavior observed across the MTJs. Density functional theory calculations (B3LYP, 6-31G*) were carried out on the gas-phase (geometry optimized) molecular wire, the HOMO–LUMO gap of which was determined to be 3.8 eV (HOMO (highest occupied molecular orbital): −5.6 eV vs. vacuum, LUMO (lowest unoccupied molecular orbital): −1.8 eV vs. vacuum; see Figure S8 in the Supporting Information). In addition, a single-level model[28] was used to fit the experimental *I–V* curve (see the Supporting Information for details). When transport in the Landauer regime of coherent tunneling was assumed,[29–31] a transport equation dominated by one channel (single-level picture) was formulated to obtain the electrode–molecule coupling (0.037 eV on both sides) and the energy gap between the Fermi level and the molecular level (0.75 eV). By taking an Au Fermi level at around 5 eV, our results indicate that hole transport (that is, through the HOMO) dominates. The experimental results (Figure 2c, ▽) and theoretical fit (Figure 2c) are in good agreement.

Multistep reactions can also be carried out within the nanogaps in a stepwise approach that is analogous to solid-phase synthesis. The ability to extend and vary the chemical structure within MTJs in situ allows the determination, in a high throughput, combinatorial fashion, of how the changes in molecular structure within the gaps affect transport properties. To this end, we have synthesized **3**, a fluorene derivative with alkyne substituents. When **3** is reacted with the available azide from **2** on the Au electrode under click reaction conditions, the oligomeric fluorene chain is extended, which either bridges the gap or leaves an azide group available for further reaction (Figure 4). The number of fluorene monomers in the oligomeric chain is controlled precisely by the number of reaction steps and the gap size. We have produced

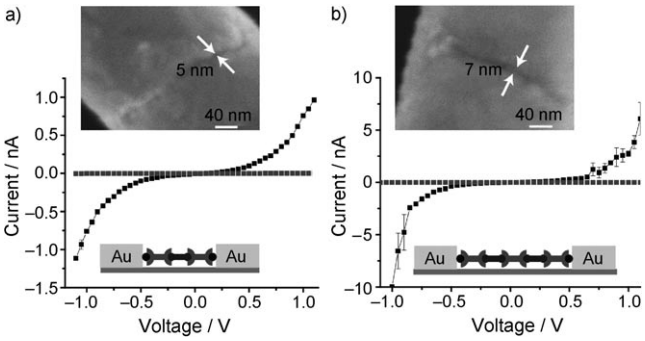

Figure 4. Representative *I–V* response curves for the multistep click reactions within OWL-fabricated gaps before and after the final click reaction step. a) 5 nm OWL-fabricated gap, two-step click reaction and b) 7 nm OWL-fabricated gap, three-step click reaction.

MTJs with three and five fluorene monomers from two and three click reaction steps in 5 and 7 nm gaps, respectively. Transport is observed only after the appropriate number of reaction steps to bridge the gap have been carried out. In the case of the 5 nm gap, no current is seen until two reactions have been carried out, and, in the case of the 7 nm gap, no current is seen until three reactions have been carried out. These experiments demonstrate the ability to carry out multiple reaction steps within the gap.

In summary, we have demonstrated a new method for the in situ, modular fabrication of MTJs through click chemistry in OWL-fabricated nanogaps, whereby the Raman enhancement inherent to these nanostructures is used to spectroscopically characterize the molecular assembly processes within the gaps. The use of click chemistry to form MTJs proceeds in

high yields and can be used to test different molecules; the resulting triazole form maintains conjugation in the molecular wires. In addition, this method overcomes a major challenge in the field of molecular electronics, that is, the ability to spectroscopically track the assembly processes of MTJs within such tiny gaps. By using the azide–alkyne click reaction to affix molecules within the gap, the transport properties of different functional building blocks can be explored. We have demonstrated this concept by synthesizing fluorene oligomers of different lengths within the gaps and studying their transport properties. We anticipate that this new method of forming and characterizing MTJs will be used to create nanoelectronic devices with diverse functions and applications.

Received: December 10, 2008
Published online: February 19, 2009

Keywords: click chemistry · fluorene · molecular electronics · nanowires · on-wire lithography

[1] A. Nitzan, M. A. Ratner, *Science* **2003**, *300*, 1384 – 1389.
[2] N. J. Tao, *Nat. Nanotechnol.* **2006**, *1*, 173 – 181.
[3] J. M. Tour, *Acc. Chem. Res.* **2000**, *33*, 791 – 804.
[4] M. Taniguchi, Y. Nojima, K. Yokota, J. Terao, K. Sato, N. Kambe, T. Kawai, *J. Am. Chem. Soc.* **2006**, *128*, 15062 – 15063.
[5] J. Y. Tang, Y. L. Wang, J. E. Klare, G. S. Tulevski, S. J. Wind, C. Nuckolls, *Angew. Chem.* **2007**, *119*, 3966 – 3969; *Angew. Chem. Int. Ed.* **2007**, *46*, 3892 – 3895.
[6] L. D. Qin, S. Park, L. Huang, C. A. Mirkin, *Science* **2005**, *309*, 113 – 115.
[7] X. D. Chen, Y. M. Jeon, J. W. Jang, L. D. Qin, F. W. Huo, W. Wei, C. A. Mirkin, *J. Am. Chem. Soc.* **2008**, *130*, 8166 – 8168.
[8] L. D. Qin, J. W. Jang, L. Huang, C. A. Mirkin, *Small* **2007**, *3*, 86 – 90.
[9] L. D. Qin, S. L. Zou, C. Xue, A. Atkinson, G. C. Schatz, C. A. Mirkin, *Proc. Natl. Acad. Sci. USA* **2006**, *103*, 13300 – 13303.
[10] L. D. Qin, M. J. Banholzer, J. E. Millstone, C. A. Mirkin, *Nano Lett.* **2007**, *7*, 3849 – 3853.
[11] G. F. Zheng, L. D. Qin, C. A. Mirkin, *Angew. Chem.* **2008**, *120*, 1964 – 1967; *Angew. Chem. Int. Ed.* **2008**, *47*, 1938 – 1941.
[12] H. C. Kolb, M. G. Finn, K. B. Sharpless, *Angew. Chem.* **2001**, *113*, 2056 – 2075; *Angew. Chem. Int. Ed.* **2001**, *40*, 2004 – 2021.
[13] L. A. Bumm, J. J. Arnold, M. T. Cygan, T. D. Dunbar, T. P. Burgin, L. Jones, D. L. Allara, J. M. Tour, P. S. Weiss, *Science* **1996**, *271*, 1705 – 1707.
[14] X. D. Cui, A. Primak, X. Zarate, J. Tomfohr, O. F. Sankey, A. L. Moore, T. A. Moore, D. Gust, G. Harris, S. M. Lindsay, *Science* **2001**, *294*, 571 – 574.
[15] B. Q. Xu, N. J. Tao, *Science* **2003**, *301*, 1221 – 1223.
[16] J. G. Kushmerick, D. B. Holt, S. K. Pollack, M. A. Ratner, J. C. Yang, T. L. Schull, J. Naciri, M. H. Moore, R. Shashidhar, *J. Am. Chem. Soc.* **2002**, *124*, 10654 – 10655.
[17] M. A. Reed, C. Zhou, C. J. Muller, T. P. Burgin, J. M. Tour, *Science* **1997**, *278*, 252 – 254.
[18] J. Reichert, R. Ochs, D. Beckmann, H. B. Weber, M. Mayor, H. von Lohneysen, *Phys. Rev. Lett.* **2002**, *88*, 176804.
[19] D. L. Pearson, J. M. Tour, *J. Org. Chem.* **1997**, *62*, 1376 – 1387.
[20] L. T. Cai, Y. X. Yao, J. P. Yang, D. W. Price, J. M. Tour, *Chem. Mater.* **2002**, *14*, 2905 – 2909.
[21] D. J. V. C. van Steenis, O. R. P. David, G. P. F. van Strijdonck, J. H. van Maarseveen, J. N. H. Reek, *Chem. Commun.* **2005**, 4333 – 4335.
[22] D. G. Castner, K. Hinds, D. W. Grainger, *Langmuir* **1996**, *12*, 5083 – 5086.
[23] J. P. Collman, N. K. Devaraj, T. P. A. Eberspacher, C. E. D. Chidsey, *Langmuir* **2006**, *22*, 2457 – 2464.
[24] J. H. Tian, B. Liu, X. L. Li, Z. L. Yang, B. Ren, S. T. Wu, N. J. Tao, Z. Q. Tian, *J. Am. Chem. Soc.* **2006**, *128*, 14748 – 14749.
[25] D. R. Ward, N. J. Halas, J. W. Ciszek, J. M. Tour, Y. Wu, P. Nordiander, D. Natelson, *Nano Lett.* **2008**, *8*, 919 – 924.
[26] G. Braun, I. Pavel, A. R. Morrill, D. S. Seferos, G. C. Bazan, N. O. Reich, M. Moskovits, *J. Am. Chem. Soc.* **2007**, *129*, 7760 – 7761.
[27] B. K. Yoo, S. W. Joo, *J. Colloid Interface Sci.* **2007**, *311*, 491 – 496.
[28] S. Yeganeh, M. Galperin, M. A. Ratner, *J. Am. Chem. Soc.* **2007**, *129*, 13313 – 13320.
[29] R. Landauer, *IBM J. Res. Dev.* **1957**, *1*, 223 – 231.
[30] R. Landauer, *Philos. Mag.* **1970**, *21*, 863 – 867.
[31] Y. Meir, N. S. Wingreen, *Phys. Rev. Lett.* **1992**, *68*, 2512 – 2515.

